Physics   College of Arts and Sciences

2009

Transit Time Measurements of Charge Carriers in Disordered Silicons: Amorphous, Nanocrystalline, and Nanoporous

Eric A. Schiff
Syracuse University

Follow this and additional works at: http://surface.syr.edu/phy
Part of the Physics Commons

Taylor & Francis
Taylor & Francis Group

Transit-time measurements of charge carriers in disordered silicons: Amorphous, microcrystalline and porous

E.A. Schiff*

Department of Physics, Syracuse University, Syracuse, NY 13244-1130, USA

We summarize published hole transit-time measurements for hydrogenated amorphous silicon, microcrystalline silicon, and light-emitting nanoporous silicon in terms of drift mobilities and dispersion parameters. For amorphous and microcrystalline silicon, the anomalously dispersive measurements are broadly consistent with multiple-trapping by bandtail traps with an exponential distribution of energy depths. One unexplained result has been that the trap emission prefactor frequency ν is about 1000 times smaller in microcrystalline silicon than in amorphous silicon. We present a model incorporating both detailed-balance effects and a previously proposed Meyer–Neldel variation of ν with trap-depth; the model accounts for the factor 1000. We discuss general trap distributions incorporating variations of both trap depth and prefactor frequency; a model for which dispersion is due entirely to prefactor variation accounts for measurements on nanoporous silicon.

Keywords: a-Si:H; microcrystalline silicon; mobility; porous silicon

1. Introduction

In 1957, Walter Spear published a seminal paper: *Transit-time measurements of charge carriers in amorphous selenium* [1]. His measurements were the first reasonably direct observation of the drift velocity of charge carriers in an amorphous semiconductor and were among the first such measurements in any material. Since those early measurements, transit-time or 'time-of-flight' measurements have become quite important in non-crystalline and nanocrystalline materials. Charge carrier drift is typically much slower than for crystalline materials, which makes the transit-times relatively easy to measure (even with 1950s electronics). The physics of this slow drift is subtler than the effective-mass ideas that are usually applied in crystals and this new physics has also largely precluded substituting Hall-effect measurements for direct transit-time studies. Finally, slow charge carrier drift proves to be intrinsically important in devices such as solar cells and thin-film transistors.

Spear is now known best not as the inventor of transit-time measurements but as the discoverer of the important properties of hydrogenated amorphous silicon (a-Si:H). These properties are presently being exploited on an enormous scale in displays, televisions and solar cells, but among the first measurements suggesting

*Email: easchiff@syr.edu

them were Peter LeComber and Walter Spear's transit-time measurements [2]. LeComber and Spear speculated from their measurements that electron drift in a-Si:H was determined by a disorder-limited band mobility μ of magnitude 1–$10\,\mathrm{cm^2\,V^{-1}\,s^{-1}}$ and by localized traps that captured and re-emitted the electrons. Their speculation proved to be correct in essence. It was later articulated in much greater detail in terms of exponential distributions of traps tailing away from the bandedges, which leads to a strongly temperature-dependent form of 'anomalously dispersive' transport [3,4]. Bandtails are now recognized as a common feature of disordered materials and, for a-Si:H and related materials, we now know how the bandtail widths are affected by germanium alloying and by incipient crystallinity. We also know that the band mobility μ is surprising unaffected by these changes. However, the bandtail trapping model is phenomenological: we still cannot predict either the bandtail widths or the band mobility from deeper considerations.

One aspect of bandtail trapping that has received relatively little consideration will be the primary focus of the present paper. This aspect is the frequency prefactor ν that governs the activated emission rate e from a trap: $e = \nu \exp(-E_\mathrm{a}/k_\mathrm{B}T)$, where E_a is the activation energy and $k_\mathrm{B}T$ is the thermal energy. For many years, ν appeared to be essentially a constant around $10^{12}\,\mathrm{s^{-1}}$ for bandtail traps in these varying materials. However, recent measurements on holes indicate that ν declines by about 10^3 as a-Si:H is transformed into microcrystalline silicon (μc-Si:H) [5,6].

In this paper we describe two mechanisms that contribute to this effect. First, as crystallinity is approached, the effective density-of-states N_V at the valence bandedge gets smaller by perhaps 20 times its value in a-Si:H. A detailed-balance argument suggests that ν is proportional to N_V; while the sign of the effect agrees with the measurements, the magnitude is too small to completely explain the measured change of 10^3. Second, at least two groups have proposed that ν varies exponentially with trap depth. Kagawa and Matsumoto [7][1] suggested that deeper bandtail states have substantially smaller values for ν than shallower states. Chen et al. [8] have suggested that the deeper states have much larger values for ν than shallow states; we term their proposal the 'Meyer–Neldel' proposal. We show that the combination of both the detailed-balance and the Meyer–Neldel proposals can account for the change in ν between a-Si:H and μc-Si:H. The Meyer–Neldel proposal has the virtue that it is consistent with experience for deep traps, but it does lead to difficulties in interpreting optical and photoemission estimates of the valence bandtail width.

We conclude by considering two-dimensional distributions of trap depths and emission prefactors. We illustrate this idea for Meyer–Neldel behavior and then for the general situation in which there may be a broad distribution of values for ν even among traps with a common depth. This latter possibility can predict temperature-independent dispersion, which is characteristic of light-emitting nanoporous silicon and other porous materials. We speculate that these distributions may be typical for disordered, porous materials in general.

2. Transit-time measurements

In the 1950s, pulse electronics began to be applied to measuring carrier motions in insulators, and in 1957 Walter Spear published the first 'transit time' measurements
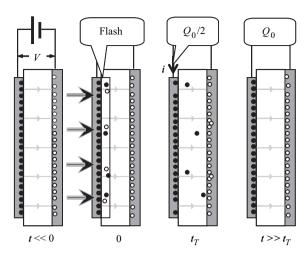
Figure 1. Cartoon illustrating Walter Spear's transit-time experiment as adapted for anomalously dispersive transport.

on thin-film amorphous selenium (a-Se). Figure 1 is a cartoon to illustrate the method. The leftmost panel of the figure illustrates that the sample can be viewed essentially as the dielectric in a parallel plate capacitor; no significant currents flow in the dark. In the second panel, a short flash of light or of electrons that arrives at time $t = 0$ has excited a thin layer of material; equal magnitudes of charge Q_0 of electrons and holes have been generated. The cartoon also indicates that the magnitude of the charge that is generated is less than the initial charge on the electrodes. This is a common experimental precaution to make sure the internal electric field is not changed substantially by the generated charge. The third panel labeled t_T is worth studying; it corresponds to a snapshot of the time at which the average displacement of holes is halfway across the insulator. The original charge $-Q_0$ of electrons (open symbols) rapidly recombined with positive charges on the electrode to the left. A photocurrent has been flowing through the external bias circuit since $t = 0$ to maintain the electric potential V despite the motion of the holes in the material; by the time t_T, a charge $Q_0/2$ has flowed through the external circuit. As can be seen, the charge on the left electrode is reduced by $Q_0/2$; the right electrode's charge has become still more negative (by $-Q_0/2$), and the balancing positive charge Q_0 is stored in the insulator. Once the holes have all arrived at the right-hand electrode, the total charge that has flowed through the external circuit reaches Q_0.

Figure 2 replots some of Spear's original transit-time measurements for holes in a-Se [1], along with some much later measurements for electrons in hydrogenated amorphous silicon (a-Si:H). The horizontal axis corresponds to the transit-times. Spear defined the transit time as the time for full collection of charge, which corresponds to a displacement $L = d$, where d is the thickness of the film. The vertical axis L/F is the ratio of the displacement L to the field $F = V/d$. As can be seen, Spear's measurements on a-Se are an elegant confirmation of the simplest 'drift-velocity' view of hole motion $v_D = \mu_D F$, where v_D is the drift-velocity, F is the
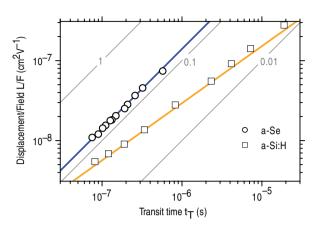
Figure 2. Transit-time measurements for holes in a-Se at 293 K [1] and for electrons in a-Si:H at 157 K [4]. The vertical axis is the (varying) ratio of the carriers' displacement L to the electric field F. The thin gray lines indicate the L/F versus t_T relation for drift mobilities of 1, 0.1 and 0.01 cm^2 V^{-1} s^{-1}.

electric field and μ_D is the drift-mobility. Even on double-logarithmic scales, his measurements show a near-perfect proportionality of the hole displacement/field ratio L/F upon the transit-time t_T:

$$L/F = \mu_D t_T. \tag{1}$$

The thin gray lines in the figure illustrate this relation for the values $\mu_D = 1$, 0.1 and 0.01 cm^2 V^{-1} s^{-1}.

The first transit time measurements on a-Si:H were done in 1970 by LeComber and Spear [2], who were discovering the remarkable properties of this material. In Figure 2, we show the later, more mature measurements on electrons by Marshall et al. [4]. We explain the details momentarily, but notice that they do not exhibit proportionality of L/F and t_T; instead the displacement/field ratio rises as an odd power-law with time:

$$L/F \propto (t_T)^{\alpha}. \tag{2}$$

These data are one aspect of a phenomenon called 'anomalously dispersive transport' that was discovered around 1975 by Harvey Scher and his collaborators [9]; the power-law α is called the 'dispersion parameter', where ordinary transport (with Gaussian dispersion) corresponds to $\alpha = 1$. LeComber and Spear did not know about anomalous dispersion in 1970, which is why we have used later work to illustrate the effect.

Anomalous dispersion requires a thorough revision of the treatment of transit-time experiments. For normally dispersive transport, the sheet of holes in a transit-time experiment moves through the material with little spreading, and arrives at the opposing electrode at a well-defined transit-time corresponding to a displacement $L = d$, where d is the thickness of the layer. For anomalous dispersion, there is no well-defined time at which charge collection is complete, and so the transit-time t_T is typically redefined in terms of half-charge collection or closely related measures;
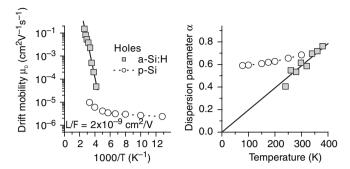
Figure 3. Temperature-dependent hole drift properties for representative samples of amorphous silicon [10] and porous silicon [11]. Hole transport in both systems is dispersive, and the right panel shows the temperature-dependent dispersion parameter α. The left panel shows the drift mobilities for a displacement-field ratio $L/F = 2 \times 10^{-9} \, \mathrm{cm^2 \, V^{-1}}$.

we have used the half-charge definition in Figure 1. Although we do not prove it here, the displacement L of the mean position of the carriers is $d/2$ with this modified definition of t_{T} [12]. As illustrated in Figure 1, for anomalously dispersive transport the carriers are not distributed as a well-defined sheet at t_{T}, but are smeared throughout the thickness of the sample. Returning to Figure 2, note that the drift-mobility, defined as $\mu_{\mathrm{D}} = L/Ft_{\mathrm{T}}$, is not just a constant for all displacement/field ratios L/F for the anomalously dispersive a-Si:H data. For the measurements shown, μ_{D} falls from $0.1 \, \mathrm{cm^2 \, V^{-1} \, s^{-1}}$ for small L/F to 0.01 for large values.

For dispersive transport systems, a reasonably compact description of drift-mobility measurements is a pair of graphs showing the temperature-dependent drift-mobility μ_{D} for a convenient value of L/F, and the corresponding temperature-dependent dispersion parameter. This recipe has been followed in Figure 3, which presents measurements on holes for two additional systems that exhibit strong dispersion: holes in a-Si:H [10] and holes in light-emitting nanoporous silicon [11]. For holes in a-Si:H, the mobility and dispersion parameter show strongly temperature-dependent behavior and in the next section we describe the bandtail trapping model for this. For porous silicon, both the mobility and the dispersion parameter are weakly dependent on temperature; we will return to this behavior in the last section of the paper.

For dispersive transport systems such as a-Si:H, the drift-mobility μ_{D} depends upon the particular ratio L/F of the carrier's displacement L to the electric field E. The implication is that drift-mobilities in differing samples must be compared at a common value for L/F [12], as has been done in Figure 3. The dependence of μ_{D} on L/F is sometimes misinterpreted as suggesting that dispersive transport is nonlinear with electric field, which is not generally true. For a given time lapse since the carriers were photogenerated, the mean displacement L is usually proportional to F.

3. Exponential bandtails and the standard multiple-trapping model

Measurements of the temperature-dependence and the dispersion of photocarrier drift mobilities in a-Si:H and related materials are often well described by a 'bandtail
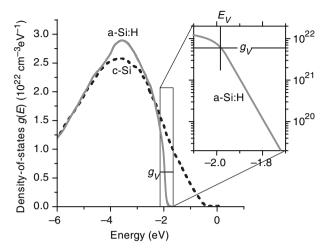
Figure 4. Electronic density-of-states for a-Si:H and c-Si:H inferred from ultraviolet photoemission measurements [14]. The inset shows the exponential tailing for a-Si:H, as well as the location of the bandedge proposed separately by Liang et al. [15].

multiple-trapping model'. The model itself and its early successes were reviewed some time ago [3,13]. Drift-mobility and transport researchers continue to debate the range of its application and the fundamental meaning of its parameters, as indeed we are doing in the present paper.

The model originates with the fact that the electronic density-of-states in a-Si:H near the bandedges falls exponentially. In Figure 4, we have illustrated the density-of-states in a-Si:H and crystal silicon (c-Si) as inferred from an ultraviolet photoemission experiment [14]. There is a very steep decline of the density-of-states for a-Si:H that sets in at about $10^{22}\,\mathrm{cm^{-3}\,eV^{-1}}$, and that is exponential over several orders of magnitude (see inset).

The multiple-trapping model assumes the existence of a well-defined bandedge or mobility-edge separating delocalized transport states (below E_V) and localized traps (above E_V). We have illustrated a location for the mobility-edge E_V in Figure 4 that is consistent with the original reference and also with much later solar cell device modeling [15].

In its simplest form, the multiple-trapping model uses three parameters to fit drift-mobility measurements [6]. For holes, these are:

ΔE_V: the width of the exponential valence bandtail
μ_p: the mobility of free holes in levels below E_V
v: the frequency prefactor for the emission of holes from bandtail traps.

In this model, emission of holes from bandtail traps is described by the equation $e = v\exp(-(E - E_V)/k_B T$, where E is the level energy of the bandtail state and v is the 'emission prefactor frequency' (often referred to as the 'attempt-to-escape frequency'). The hallmark of exponential bandtail trapping is that the dispersion parameter α should be proportional to the temperature: $\alpha = k_B T/\Delta E_V$, which is reasonably consistent with most experiments and with Figure 3.[2]
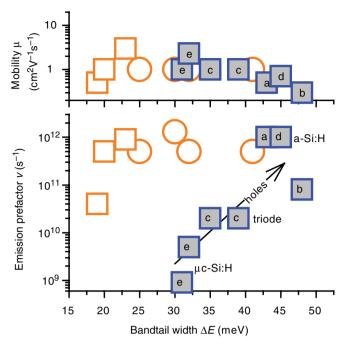
Figure 5. Exponential bandtail parameters obtained from conventional multiple-trapping fits to drift-mobility measurements in a-Si:H, a-SiGe:H and μc-Si:H samples. Open symbols indicate electrons; closed symbols indicate holes; circular symbols represent silicon-germanium alloys. Based on data in [6].

Measurements of hole drift published by several groups for a-Si:H and μc-Si:H have been fitted using the simplest exponential bandtail multiple-trapping model, with the results shown as the filled symbols in Figure 5. The letters inside the symbols indicate the original experimental papers (a [3], b [10], c [16], d [17], e [5]). The fittings are not from the original papers, but from [6]; fitting parameters do depend on the particular variation of the multiple-trapping model that is used, which explains why it was necessary to refit the measurements from the several different groups using a single model. For reference, results for electrons have been shown as open symbols without keys; conduction bandtail widths larger than 25 meV are due to Ge alloying. Not all published data on hole and electron mobilities is included; see [6] for a full discussion.

The band mobilities fitted from the experiments are about $1 \, cm^2 \, V^{-1} \, s^{-1}$. This result suggests that the mobility-edge has similar properties for a wide range of samples and measurements. It applies to holes in samples with structures ranging from amorphous to nanocrystalline. It applies to both electrons and holes. For electrons, it applies in both silicon and a range of silicon-germanium alloys. In addition, while the measurements summarized by Figure 5 were nanosecond domain measurements, picosecond domain measurements give the same magnitude. Considered together, these multiple results suggest that the band mobility is a universal property of the mobility-edge in this class of disordered materials.

In his original treatment of a mobility-edge, Mott [18] proposed that the universal property of a mobility-edge would be a minimum metallic conductivity, which is essentially the product of the bandedge density-of-states N_V and the band mobility μ. At that time, there was very little known about the wavefunctions near a mobility-edge. Recent computational work has shown that bandedge states very near the mobility-edge have a complex, sponge-like spatial structure [18] that was not envisioned in the early analytical work. Despite this improvement in knowledge of mobility-edge properties, there is, as yet, no simple explanation for a universal mobility around $1\,\mathrm{cm^2\,V^{-1}\,s^{-1}}$.

The valence bandtail width falls from 45–50 meV for a-Si:H to $\sim$30 meV for μc-Si:H; this result seems sensible, although it is intriguing that the valence bandtail width in μc-Si:H is larger than the conduction bandtail width for a-Si:H. The most prominent change in hole drift as the material is transformed from amorphous to nanocrystalline is the bandtail emission prefactor ν, which falls nearly 1000-fold; to our knowledge, no explanation has been proposed for this effect.

4. Emission prefactor and the bandedge density-of-states

One contribution to this large change stems from the 'detailed-balance' equation that connects a trap's emission prefactor ν to the effective density-of-states at the valence bandedge N_V and the 'trapping coefficient' b_t that describes hole capture by a trap:

$$\nu = N_V b_t \tag{3}$$

Since b_t governs the capture of a hole from a level near the mobility-edge to a bandtail level above it, one might expect that universality of levels near the mobility-edge would keep b_t constant despite the change from an amorphous to a nanocrystalline solid. The fact that the band mobility fitted from multiple-trapping did not vary significantly between the two materials seems consistent with this perspective. Thus, we would expect that the changes in N_V would dominate the observed changes in ν.

For a-Si:H, both photoemission experiments [14] and solar cell device modeling [15] indicate a value $N_V \sim 4 \times 10^{20}\,\mathrm{cm^{-3}}$ near room temperature. This value is about 40 times larger than the value for the valence band in c-Si, which is $1.0 \times 10^{19}\,\mathrm{cm}$ [29]. A value of $2 \times 10^{19}\,\mathrm{cm^{-3}}$ may be an adequate approximation to the value of N_V for μc-Si:H, given that the latter has Raman-vibrational properties and optical properties more similar to c-Si than a-Si:H.

It is worth noting that these results do not support a minimum-metallic conductivity view, which is that the product $N_V e \mu_h$ should have a constant magnitude at a mobility-edge. μ_h varies little between a-Si:H and μc-Si:H, despite the changes in N_V; for a minimum metallic conductivity, μ_h should increase as N_V falls.

The change in N_V between a-Si:H and μc-Si:H accounts for – at most – a 20-fold change in ν. While this change has the right sign, a factor of 50 of the change remains unexplained.

5. Meyer–Neldel effect for emission prefactors

The conventional, bandtail multiple-trapping model that we have been using assumes that ν is constant for bandtail states of varying level energies; Figure 5 is based on this view. However, temperature-dependent emission experiments on deep-traps show large (many orders of magnitude) variations of the emission prefactors for varying traps [19]. In particular, if the emission rate as a function of temperature T is written

$$e(T) = \nu \exp(-E_A/k_B T), \qquad (4)$$

where E_A is the activation-energy, it is common to find 'Meyer–Neldel' behavior for the emission prefactors of the deep-traps in a given system:

$$\nu(E_A) = \nu_{00} \exp(E_A/E_{MN}). \qquad (5)$$

Here E_{MN} is the Meyer–Neldel energy and ν_{00} is the 'bandedge' emission prefactor. Meyer–Neldel behavior corresponds to larger emission prefactor frequencies for deeper traps; as one example, for electron emission from deep-traps in undoped a-Si:H, Antoniadis and Schiff [20] reported a Meyer–Neldel effect with $E_{MN} = 26$ meV.

The prefactor ν for a deep trap is affected by thermal shifts of the deep level relative to the bandedge, as well as by any changes in the true emission frequency. For a-Si:H, Spear et al. [21] were among the first to discuss thermal shifts, which have received a comprehensive treatment in the monograph of Overhof and Thomas [22]. Yelon et al. [19] have recently discussed the relative role of thermal shifts and true frequency changes for a wide range of Meyer–Neldel systems, and conclude that thermal shifts are unlikely to be the sole explanation for the wide range of Meyer–Neldel behavior.

For bandtail traps, which are effectively attached to the bandedge, thermal shifts should have little effect on the emission prefactor, and we shall neglect them in the remaining discussion. As noted above, nearly all workers have neglected any variation in the emission prefactor frequency for varying bandtail trap depths. However, in the early 1980s, Kagawa and Matsumoto [7][1] proposed an exponential decrease of ν with trap depth to explain some experiments that were puzzling at the time and noted that such an effect could not be excluded using time-of-flight measurements. In the late 1990s, Chen et al. [8] examined the opposite, 'Meyer–Neldel' possibility that ν increased exponentially with trap-depth, which was an extension of related work on ν for deep-traps. In particular, they proposed $E_{MN} = 70$ meV for the valence bandtail of a-Si:H [8]. They found in Monte-Carlo calculations that some of the deviations between the measurements and the conventional analysis were well explained by adding such a Meyer–Neldel dependence. Figure 6 illustrates a dependence of the emission prefactor ν on trap depth for their value of E_{MN}.

If this Meyer–Neldel view is accepted, then drift-mobility experiments that correspond to trap depths that differ substantially compared to E_{MN} will yield substantially different emission prefactor frequencies ν. This is a possible contribution to the differences in ν reported for μc-Si:H and a-Si:H. To assess the size of the contribution, we need to evaluate the typical trap-depths for the drift-mobility fittings in μc-Si:H and a-Si:H.
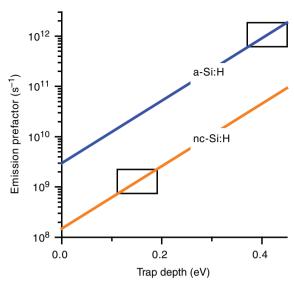
Figure 6. Emission prefactor frequency ν for varying valence bandtail trap depths based on Meyer–Neldel energy $E_{MN} = 70\,\mathrm{meV}$. The rectangular boxes roughly indicate the regions probed with hole drift-mobility measurements.

For bandtail multiple-trapping, the temperature-dependent drift-mobility has an experimental activation energy E_A that indicates the depth of the traps associated with the particular value for L/F [13]. In terms of L/F and the fitting parameters, this activation energy may be written:

$$E_A \approx \Delta E_V \ln\left(\frac{L/F}{\mu_P/\nu}\right). \tag{6}$$

For a-Si:H, typical values are $L/F = 10^{-8}\,\mathrm{cm^2\,V^{-1}}$, $\mu_p = 1\,\mathrm{cm^2\,V^{-1}\,s^{-1}}$, $\nu = 10^{12}\,\mathrm{s^{-1}}$, and $\Delta E_V = 45\,\mathrm{meV}$ [17], which yield $E_A = 410\,\mathrm{meV}$. For μc-Si:H, which has a larger hole drift-mobility, typical values are $L/F = 10^{-7}\,\mathrm{cm^2\,V^{-1}}$, $\mu_p = 1\,\mathrm{cm^2\,V^{-1}\,s^{-1}}$, $\nu = 10^9\,\mathrm{s^{-1}}$, and $\Delta E_V = 30\,\mathrm{meV}$ [5], which yield $E_A = 140\,\mathrm{meV}$. Thus hole drift-mobility measurements in a-Si:H are typically probing bandtail levels about 270 meV deeper than measurements in μc-Si:H.

If a Meyer–Neldel rule does govern valence bandtail emission, this difference in trap depth may account for a difference in the estimates of the emission prefactor. To quantify this difference, we assume that the bandedge attempt frequencies ν_{00} are proportional to the bandedge densities-of-states, so that $(\nu_{00}^{nc}/\nu_{00}^{a}) = (N_V^{nc}/N_V^{a}) \approx 0.05$. We also assume that the Chen et al. [8] estimate of $E_{MN} = 70\,\mathrm{meV}$ for the valence bandtail of a-Si:H applies to μc-Si:H as well; we discuss this assumption shortly. Given these two assumptions, we have illustrated the dependence of the emission prefactor as a function of bandtail trap depth for μc-Si:H and for a-Si:H in Figure 6. The boxes drawn in the figure indicate the attempt-frequencies corresponding to typical trap depths for drift-mobility measurements in μc-Si:H and a-Si:H. As can be seen, a Meyer–Neldel perspective, modified to account for the differing bandedge

densities-of-states, is consistent with the emission prefactor frequencies reported for hole drift-mobility measurements in μc-Si:H and a-Si:H.

We have assumed that the Meyer–Neldel energy should be similar for amorphous and for microcrystalline silicon. Comparable Meyer–Neldel energies for amorphous and microcrystalline chalcogenide films have recently been reported by Savransky and Karpov [23]. This is consistent with the 'multi-excitation entropy' (MEE) mechanism for Meyer–Neldel behavior proposed in 1990 by Yelon and Movaghar [24]. In brief, carrier emission from deeper traps occurs through the absorption of several phonons (or excitations). Both the change in the energy of the phonon system and of its entropy affect the trap emission rate, which is calculated from the change in the free-energy U–TS that is associated with carrier emission:

$$e(T) = \nu_{00} \exp(-(\Delta U - T\Delta S)/k_B T) = \nu_{00} \exp(\Delta S/k_B) \exp(-\Delta U/k_B T). \quad (7)$$

The multi-excitation entropy change is roughly $\Delta S \approx k_B \Delta U/E_E$, where E_E is a typical excitation energy; this form leads to a Meyer–Neldel rule with $E_{MN} \sim E_E$. The value $E_{MN} = 70\,\text{meV}$ proposed for valence bandtail traps has the same magnitude as the well-studied optic phonon band near 60 meV in both a-Si:H and μc-Si:H; Raman scattering of this band is commonly used to ascertain the extent of crystallinity in these materials [25].

6. Discussion

For deep level emission and, indeed, for many other phenomena with large activation energies, Meyer–Neldel effects are a commonplace observation, and multi-excitation entropy and related ideas are widely discussed. Despite the widespread applications for deep levels, these ideas have not penetrated significantly into discussions of drift-mobilities and bandtail trap models beyond the pioneering paper of Chen et al. [8]. There are at least two reasons. First, most workers have obtained fairly similar emission prefactors of $\sim 10^{12}\,\text{s}^{-1}$ when they fitted their drift mobilities to the conventional model. Their experience has thus been very different than the experience for deep levels, where enormous prefactor variations are observed. The relatively low emission prefactor estimates for hole drift mobilities that we are discussing here are fairly recent. Second, optical and photoemission studies of the valence bandtail often indicate widths of 45–55 meV, which are fairly similar to those inferred from the conventional hole drift mobility analysis [26–28]. Chen et al. [8] obtained a width of 35 meV from their Meyer–Neldel fitting, which is significantly smaller than found in the optical studies.

If a Meyer–Neldel energy of 70 meV does apply to the valence bandtail, the optical and photoemission results must have been significantly overestimating the bandtail widths. It is not difficult to find ad hoc rationalizations for overestimation: photoemission characterizes only a near-surface region, and optical measurements have different sensitivity to the spatial scale of disorder than does hole transport. Still, the present finding that low values for the emission prefactor in μc-Si:H are consistent with Meyer–Neldel behavior for bandtails may be the first surprising result. The Meyer–Neldel modification to bandtail trapping will need additional successes before it is likely to displace the conventional model.
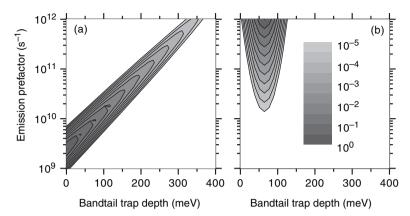
Figure 7. Contour plots of the probability densities for bandtail traps for varying trap depths and emission prefactors v; the densities are normalized to their maximum values. (a) Exponential bandtail traps calculated for a bandtail width $\Delta E_V = 35$ meV, a Meyer–Neldel energy $E_{MN} = 70$ meV and $v_{00} = 3 \times 10^9$ s^{-1}. A Gaussian broadening has been included ($\delta = 1.4$). (b) Traps with a distribution of emission prefactors yielding $\alpha = 0.6$ (as for porous silicon) and a Gaussian distribution of depths ($E_t = 60$ meV, $\delta E = 18$ meV).

The Meyer–Neldel perspective on bandtail trap emission can be generalized in a way that may help account for measurements on materials such as porous silicon. In Figure 7, we show a contour plot of the two-dimensional probability density:

$$P(E, \ln(v)) \propto \exp(-E/\Delta E_V) \exp\left(-(\ln(v) - \ln(v_{00}) - (E/E_{MN}))^2/\delta^2\right) \qquad (8)$$

that is consistent with the Meyer–Neldel behavior for a-Si:H shown in Figure 6. For convenience, we have assumed a Gaussian distribution of $\ln(v)$ for each trap depth E, with a dimensionless broadening parameter δ. With these axes, the conventional bandtail trapping model with a constant v would have a similar set of contours stretching horizontally across the plot from value v on the left axis.

This type of plot suggests that one consider more general two-dimensional distributions in which emission prefactors vary substantially even for a single trap depth. The right panel of Figure 7 illustrates this situation: there is a broad distribution of emission prefactors for distribution of trap depths tightly centered at $E_a = 60$ meV. The distribution function plotted in this panel is

$$P(E, \ln(v)) \propto \exp(\alpha \ln(v/v_{00})) \exp(-(E - E_t)^2/(\delta E)^2). \qquad (9)$$

The distribution generates a drift-mobility with temperature-independent dispersion α (Appendix 1) and it, thus, offers a possible explanation for the weak temperature-dependence of dispersive transport in porous silicon (see Figure 3).

For such traps in a porous material, the distribution of emission prefactors would not originate in multi-excitation entropy. On the other hand, in porous silicon, it seems plausible that trap states may be pushed out into the pores of the material; the emission prefactor distribution would then correspond to the distribution of tunneling rates between these localized trap states in the pores and a band of transport states. It is conceivable that these traps are related to the 'chromophores'

in porous silicon, which are the nanostructures in the material where charge carriers are trapped long enough for luminescence to occur at room-temperature.

Acknowledgements

Notes

1. The authors of [7] were influenced by a paper that measured multiphonon relaxation of rare-earth defects (L.A. Riseberg and H.W. Moos, Phys. Rev. 174 (1968) p.429). The relaxation rate decreased exponentially with the magnitude of the total phonon energy. To our knowledge, there has been no published discussion of this effect in the context of Meyer–Neldel behavior.
2. There are several methods for obtaining a dispersion parameter from time-of-flight measurements. The method of Figure 2 is merely one of these, and the reader is referred to the reviews in [3] and [13] for a more complete treatment. For a given sample, the differing methods often yield somewhat different values that presumably indicate limitations to the simplest bandtail multiple-trapping picture.

References

[1] W.E. Spear, Proc. Phys. Soc. B 70 (1957) p.669.
[2] P.G. LeComber and W.E. Spear, Phys. Rev. Lett. 25 (1970) p.509.
[3] T. Tiedje, *Time-resolved charge transport*, in *Hydrogenated Amorphous Silicon*, Vol. 2, J.D. Joannopoulos and G. Lucovsky eds., Springer, New York, 1984, p.261.
[4] J.M. Marshall, R.A. Street and M.J. Thompson, Phil. Mag. B 54 (1986) p.51.
[5] T. Dylla, F. Finger and E.A. Schiff, Appl. Phys. Lett. 87 (2005) p.032103.
[6] E.A. Schiff, J. Phys. Condens. Matter 16 (2004) p.S5265.
[7] T. Kagawa and N. Matsumoto, Phil. Mag. B 51 (1985), p.273.
[8] W.-C. Chen, L.-A. Hamel and A. Yelon, J. Non-Cryst. Solid. 200 (1997) p.254.
[9] H. Scher and E.W. Montroll, Phys. Rev. B 12 (1975) p.2455.
[10] Q. Gu, Q. Wang, E.A. Schiff, Y.-M. Li and C.T. Malone, J. Appl. Phys. 76 (1994) p.2310.
[11] P.N. Rao, E.A. Schiff, L. Tsybeskov and P. Fauchet, Chem. Phys. 284 (2002) p.129.
[12] Q. Wang, H. Antoniadis, E.A. Schiff and S. Guha, Phys. Rev. B 47 (1993) p.9435.
[13] J.M. Marshall, Rep. Prog. Phys. 46 (1983) p.1235.
[14] W.B. Jackson, S.M. Kelso, C.C. Tsai, J.W. Allen and S.-J. Oh, Phys. Rev. B 31 (1985) p.5187.
[15] J. Liang, E.A. Schiff, S. Guha, B. Yan and J. Yang, Appl. Phys. Lett. 88 (2006) p.063512.
[16] G. Ganguly, I. Sakata and A. Matsuda, J. Non-Cryst. Solid. 198/200 (1995) p.300.
[17] S. Dinca, G. Ganguly, Z. Lu, E.A. Schiff, V. Vlahos, C.R. Wronski, and Q. Yuan, *Proceedings of Amorphous and Nanocrystalline Silicon Based Films–2003*, J.R. Abelson, G. Ganguly, H. Matsumura, J. Robertson and E.A. Schiff, eds., Materials Research Society, Pittsburgh, PA, 2003, p.345.
[18] J.J. Ludlam, S.N. Taraskin, S.R. Elliott and D.A. Drabold, J. Phys. Condens. Matter 17 (2005) p.L321.
[19] A. Yelon, B. Movaghar and R.S. Crandall, Rep. Prog. Phys. 69 (2006) p.1145.

[20] H. Antoniadis and E.A. Schiff, Phys. Rev. B 46 (1992) p.9482.
[21] W.E. Spear, D. Allan, P.G. LeComber and A. Ghaith, Phil. Mag. B 41 (1980) p.419.
[22] H. Overhof and P. Thomas, *Electronic Transport in Hydrogenated Amorphous Semiconductors*, Springer, New York, 1989.
[23] S.D. Savransky and I.V. Karpov, in *Phase-Change Materials for Reconfigurable Electronics and Memory Applications*, A.H. Edwards, P.J. Fons, S. Raoux, P.C. Taylor, M. Wuttig, eds., Materials Research Society, Symp. Proc. 1072E, 2008, p.1072-G06-09.
[24] A. Yelon and B. Movaghar, Phys. Rev. Lett. 65 (1990) p.618.
[25] L. Houben, M. Luysberg, P. Hapke, R. Carius, F. Finger and H. Wagner, Phil. Mag. A 77 (1998) p.1447.
[26] T. Tiedje, B. Abeles and J.M. Cebulka, Solid State Commun. 47 (1983) p.493.
[27] L. Ley, J. Non-Cryst. Solid. 114 (1989) p.238.
[28] J.A. Howard and R.A. Street, Phys. Rev. B 44 (1991) p.7935.
[29] M. Pawlik, D. Schechter and K.H. Nicholas, *Properties of Crystalline Silicon* (R. Hull, ed.) Institution of Engineering and Technology, Stevenage, 1999, p.145.

Appendix 1. Emission prefactor distribution and dispersion

Let $s \equiv \ln(\nu/\nu_{00})$, where ν is the emission prefactor of a trap and ν_{00} is a cutoff frequency. The distribution of s that yields dispersive transport can be obtained by transforming the standard result that an exponential bandtail yields dispersive transport. The emission e from a trap with energy depth E and emission prefactor ν is

$$e/\nu_{00} = \exp(s)\exp(-E/k_\mathrm{B}T).$$

It is well established (for review, see [3]) that multiple-trapping in an exponential distribution of trap depths,

$$g(E) = g_\mathrm{v}\exp(-E/\Delta E_\mathrm{v}) = g_\mathrm{v}\exp(-\alpha E/k_\mathrm{B}T),$$

yields dispersive transport with parameter $\alpha = k_\mathrm{B}T/\Delta E_\mathrm{v}$. A corollary is that dispersive transport also obtains for an exponential distribution of s:

$$g(s) = g_\mathrm{p}\exp(\alpha s),$$

which is the result used in plotting Figure 7. g_p is the density of traps.